

# $h/2e$ Oscillations and Quantum Chaos in Ballistic Aharonov-Bohm Billiards

Shiro Kawabata\* and Katsuhiro Nakamura

*Department of Applied Physics, Osaka City University, Sumiyoshi-ku, Osaka 558, Japan*

We study the quantum interference effect for the single ballistic Aharonov-Bohm billiard in the presence of a weak magnetic field  $B$ . The diagonal part of the wave-number averaged reflection coefficient  $\delta\mathcal{R}_D$  is calculated by use of semi-classical scattering theory. In addition to the appearance of " $h/2e$  oscillation" that are caused by interference between time-reversed coherent backscattering classical trajectories,  $B$  in the conducting region leads to negative magnetoresistance and dampening of the  $h/2e$  oscillation amplitude. The  $B$  dependence of the results reflects the underlying classical (chaotic and regular) dynamics.

PACS numbers: 05.45.+b, 03.65.Sq, 73.20.My, 73.20.Fz

## I. INTRODUCTION

Recently, the interplay of chaos and quantum interference in *ballistic* quantum dots has intrigued experimentalists and theorists alike. The quantum interference effects, *e.g.*, ballistic weak localization (BWL) [1] and ballistic conductance fluctuation [2] in such structures depend on whether the underlying classical dynamics is regular or chaotic. Therefore, these effects are interesting from the viewpoint of the theory of *quantum chaos* [3].

More recently, we predicted that  $h/2e$  oscillation of magnetoconductance, analogous to Altshuler-Aronov-Spivak (AAS) effect [4] in disordered systems [5], should be observable in a single *ballistic* Aharonov-Bohm ring (hereafter called AB billiard) with magnetic flux penetrating *only* through the hollow [6]. This phenomenon of conductance oscillation is caused by the interference between a pair of time-reversed coherent back-scattering classical paths that wind the center obstacle in the billiard. We calculated the diagonal part of the BWL correction to the wave-number averaged reflection coefficient by use of semiclassical scattering (SCS) theory [1,2,7]. Our analysis [6] yielded for the *chaotic* AB billiard

$$\delta\mathcal{R}_D(\Phi) \sim \sum_{n=1}^{\infty} \exp(-\delta n) \cos\left(4\pi n \frac{\Phi}{\Phi_0}\right), \quad (1)$$

where  $\Phi_0 = h/e$  is the magnetic flux quantum and  $\Phi$  is the magnetic flux that penetrates the hollow. In eq. (1)  $\delta = \sqrt{2T_0\gamma/\alpha}$ , where  $\alpha$ ,  $T_0$ , and  $\gamma$  are system-dependent constants and correspond to the variance of the winding number distribution [8], the dwelling time for the shortest classical orbit and the escape rate [7,9], respectively. In this case, the oscillation amplitude decays exponentially with increasing rank of higher harmonics  $n$ , so that the main contribution to the conductance oscillation comes from the  $n=1$  component that oscillates with the period of  $h/2e$ . By contrast, for *regular* and *mixed* (Kolmogorov-Arnold-Moser tori and chaotic sea) AB billiard, we obtained [6]

$$\delta\mathcal{R}_D(\Phi) \sim \sum_{n=1}^{\infty} F\left(z - \frac{1}{2}, z + \frac{1}{2}; -\frac{n^2}{2\alpha}\right) \cos\left(4\pi n \frac{\Phi}{\Phi_0}\right), \quad (2)$$

where  $F$  and  $\beta$  are the hypergeometric function of confluent type and the exponent of dwelling time distribution  $N(T) \sim T^{-z}$  [7,9], respectively. In eq. (2) the oscillation amplitude decays algebraically for large  $n$ , and therefore the higher-harmonics components give noticeable contribution to magnetoconductance oscillations. These discoveries indicate that *the  $h/2e$  AAS oscillation occurs in both ballistic and diffusive systems forming the AB geometry and the behavior of higher harmonics components reflects a difference between chaotic and non-chaotic classical dynamics.*

In real experiments, however, the magnetic field would be applied to the *entire* region (both the hollow and annulus) in the billiard. Thus it is indispensable to apply the SCS theory to this case, in order to see the comparison between the experimental data and theoretical prediction. In this situation, we shall envisage  $h/2e$  oscillation together with

---

\*Present address: Physical Science Division, Electrotechnical Laboratory, Umezono 1-1-4, Tsukuba, Ibaraki 305-8568, Japan  
E-mail:shiro@etl.go.jp

the negative magnetoresistance and dampening of the  $h/2e$  oscillation amplitude with increasing magnetic field. In this paper, we shall focus our attention on two-dimensional ballistic AB billiards (e.g., the insets in Fig. 1) with the magnetic flux penetrating through the entire region and calculate reflection amplitude by use of SCS theory.

## II. SEMICLASSICAL THEORY

Following Baranger, Jalabert and Stone's arguments [1,7], we start with a quantum-mechanical reflection amplitude [10]

$$r_{n,m} = \delta_{n,m} - i\hbar\sqrt{v_n v_m} \int dy \int dy' \psi_n^*(y') \psi_m(y) G(y', y, E_F), \quad (3)$$

where  $v_m$  ( $v_n$ ) and  $\psi_m$  ( $\psi_n$ ) are the longitudinal velocity and transverse wave function for the mode  $m$  ( $n$ ), respectively.  $G$  is the retarded Green's function. To approximate  $r_{n,m}$  we replace  $G$  by its semiclassical Feynman path-integral expression [11],

$$G^{sc}(y', y, E) = \frac{2\pi}{(2\pi i\hbar)^{3/2}} \sum_{s(y,y')} \sqrt{D_s} \exp \left[ \frac{i}{\hbar} S_s(y', y, E) - i\frac{\pi}{2} \mu_s \right], \quad (4)$$

where  $S_s$  is the action integral along classical path  $s$ ,  $D_s = (v_F \cos \theta')^{-1} |(\partial\theta/\partial y')_y|$ ,  $\theta$  ( $\theta'$ ) is the incoming (outgoing) angle, and  $\mu_s$  is the Maslov index. Assuming hard walls in the leads, we substitute eq. (4) into eq. (3) and carry out the double integrals by a stationary-phase approximation. Thus we obtain

$$r_{n,m} = -\frac{\sqrt{2\pi i\hbar}}{2W} \sum_{s(\bar{n}, \bar{m})} \text{sgn}(\bar{n}) \text{sgn}(i\bar{m}) \sqrt{\tilde{D}_s} \exp \left[ \frac{i}{\hbar} \tilde{S}_s(\bar{n}, \bar{m}; E) - i\frac{\pi}{2} \tilde{\mu}_s \right], \quad (5)$$

where  $W$  is the width of the hard-wall leads and  $\bar{m} = \pm m$ . The summation is over trajectories between the cross sections at  $x$  and  $x'$  with angle  $\sin \theta = \bar{n}\pi/kW$ . In eq. (5),  $\tilde{S}_s(\bar{n}, \bar{m}; E) = S_s(y'_0, y_0; E) + \hbar\pi(\bar{m}y_0 - \bar{n}y'_0)/W$ ,  $\tilde{D}_s = (m_e v_F \cos \theta')^{-1} |(\partial y/\partial \theta')_\theta|$  and  $\tilde{\mu}_s = \mu_s + u(-(\partial\theta/\partial y')'_y) + u(-(\partial\theta'/\partial y')_\theta)$ , respectively, where  $u$  is the Heaviside step function. The Kronecker delta term in eq. (3) is exactly canceled by the contributions of paths of zero length [12]. Within the diagonal approximation [1,7], the quantum correction  $\delta R$  to the classical reflection probability  $R_{cl}$ , viz.,

$$R = \sum_{n,m=1}^{N_M} |r_{n,m}|^2 \approx R_{cl} + \delta R \quad (6)$$

with the mode number  $N_M$ , is given by

$$\delta R_D = \frac{1}{2} \frac{\pi}{kW} \sum_n \sum_{s \neq u} \sqrt{\tilde{A}_s \tilde{A}_u} \exp \left[ ik \left( \tilde{L}_s - \tilde{L}_u \right) + i\pi\nu_{s,u} \right], \quad (7)$$

where  $s$  and  $u$  label the classical trajectories. In eq. (7),  $\tilde{L}_s = \tilde{S}_s/k\hbar$ ,  $\nu_{s,u} = (\tilde{\mu}_u - \tilde{\mu}_s)/2$ , and  $\tilde{A}_s = (\hbar k/W) \tilde{D}_s$ . The wave-number averaging of  $\delta R_D$  over all  $k$ , denoted as  $\delta \mathcal{R}_D$ , eliminates all paths except those that satisfy  $\tilde{L}_s = \tilde{L}_u$  in eq. (7). In the absence of spatial symmetry,  $\tilde{L}_s = \tilde{L}_u$  holds if  $u$  is the time reversal of  $s$ . A weak magnetic field does not change the classical trajectories appreciably but does change the phase difference between the time-reversed trajectories by  $(S_s - S_u)/\hbar = 2\Theta_s B/\Phi_0$ , where  $\Theta_s \equiv 2\pi \int_s \mathbf{A} \cdot d\ell/B$  is the effective area almost enclosed by the classical path. To evaluate the summation over  $s$  and  $n$ , we shall reorder the backscattering classical paths according to the increasing effective area. Therefore, we obtain

$$\delta \mathcal{R}_D(B) \sim \int_{-\infty}^{\infty} d\Theta N(\Theta) \exp \left( i\frac{2\Theta B}{\Phi_0} \right), \quad (8)$$

where  $N(\Theta)$  is the distribution of  $\Theta$ . The phenomenological statistical theory leading to a distribution of the enclosed area  $N(\Theta)$  for chaotic AB billiards is given as follows. There exist two kind of classical paths and  $N(\Theta)$  is the sum of the distribution of unwinding trajectories, viz.,  $N_0(\Theta)$  and that of  $n$  ( $n \neq 0$ ) winding trajectories. This is due to

all classical trajectories winding a center obstacle  $n$  times until they exit, except for very short backscattered paths ( $n=0$  component).  $N_0(\Theta)$  is essentially the same as that of an ordinary chaotic billiard (*e.g.*, stadium), obeying a monotonic exponential law [7,9], *i.e.*,  $N_0(\Theta) \sim \exp(-\varepsilon_{cl} |\Theta|)$ , where  $\varepsilon_{cl}$  is the inverse of the average area enclosed by classical trajectories. Therefore, the full distribution of the enclosed area is given by

$$N(\Theta) \sim N_0(\Theta) + \sum_{\substack{n=-\infty \\ n \neq 0}}^{\infty} N(\Theta, n)P(n), \quad (9)$$

where  $P(n)$  and  $N(\Theta, n)$  are the distribution of the winding number  $n$  and that of the enclosed area for a given  $n$ , respectively. Owing to the ergodic properties of fully chaotic systems,  $N(\Theta, n)$  is assumed to obey a Gaussian distribution in which the variance of area is proportional to  $n$ , *i.e.*,

$$N(\Theta, n) \sim \frac{1}{\sqrt{2\pi\beta|n|}} \exp \left[ -\frac{(\Theta - n\Theta_0)^2}{2\beta|n|} \right]. \quad (10)$$

On the other hand, exploiting Berry and Keating's argument [8],  $P(n)$  is given by

$$P(n) = \int_0^{\infty} dT P(n, T) N(T) \sim \exp(-\delta|n|), \quad (11)$$

where  $\delta = \sqrt{2T_0\gamma/\alpha}$ . In eq.(11),  $N(T) \sim \exp(-\gamma T)$  and

$$P(n, T) = \sqrt{\frac{T_0}{2\pi\alpha T}} \exp \left( -\frac{n^2 T_0}{2\alpha T} \right) \quad (12)$$

are the exponential dwelling time distribution [7,9] and the Gaussian distribution of winding numbers  $n$  for trajectories with a fixed  $T$  [6,8], respectively. With the use of eqs.(10) and (11), we reach

$$N(\Theta) \sim A e^{-\varepsilon_{cl}|\Theta|} + \sum_{\substack{n=-\infty \\ n \neq 0}}^{\infty} \frac{1}{\sqrt{2\pi\beta|n|}} \exp \left[ -\frac{(\Theta - n\Theta_0)^2}{2\beta|n|} - \delta|n| \right]. \quad (13)$$

To examine the validity of expression (13), we directly calculated  $N(\Theta)$  for chaotic AB billiards (a single Sinai billiard [13]) by mean of classical numerical simulations. In the calculations, we inject  $10^8$  particles into the billiard at different initial conditions.  $N(\Theta)$  for the chaotic AB billiard has proved to be nicely fitted by eq. (13) [see Fig. 1(a)]. (In this case,  $\Theta_0/2\pi$  is approximately the average area between the outer square and inner circles.) As the size of center obstacle approaches zero, the Sinai geometry becomes square (regular billiard). In this case, we have confirmed that the oscillation structure disappears and  $N(\Theta)$  obeys a well-known power law [7,9]. Substituting eq. (13) into eq. (8), we finally obtain

$$\delta\mathcal{R}_D(\Phi) \sim \frac{A\varepsilon_{cl}^{-1}}{1 + \left( \frac{4\pi}{\Theta_0\varepsilon_{cl}} \frac{\Phi}{\Phi_0} \right)^2} + \sum_{n=1}^{\infty} \exp \left[ -\left\{ \delta + \frac{\beta}{2} \left( \frac{4\pi}{\Theta_0} \frac{\Phi}{\Phi_0} \right)^2 \right\} n \right] \cos \left( 4\pi n \frac{\Phi}{\Phi_0} \right), \quad (14)$$

where  $\Phi = B\Theta_0/2\pi$ . The first term in eq. (14), *i.e.*,  $A\varepsilon_{cl}^{-1} / \left\{ 1 + (2B/\varepsilon_{cl}\Phi_0)^2 \right\}$ , which contributes to negative magnetoresistance, agrees with Baranger, Jalabert and Stone's Lorentzian BWL correction

$$\delta\mathcal{R}_D(B) = \frac{\mathcal{R}_{cl}}{1 + \left( \frac{2B}{\varepsilon_{cl}\Phi_0} \right)^2} \quad (15)$$

for chaotic billiard [1,7], where  $\mathcal{R}_{cl}$  is the wave-number-averaged classical reflection probability.

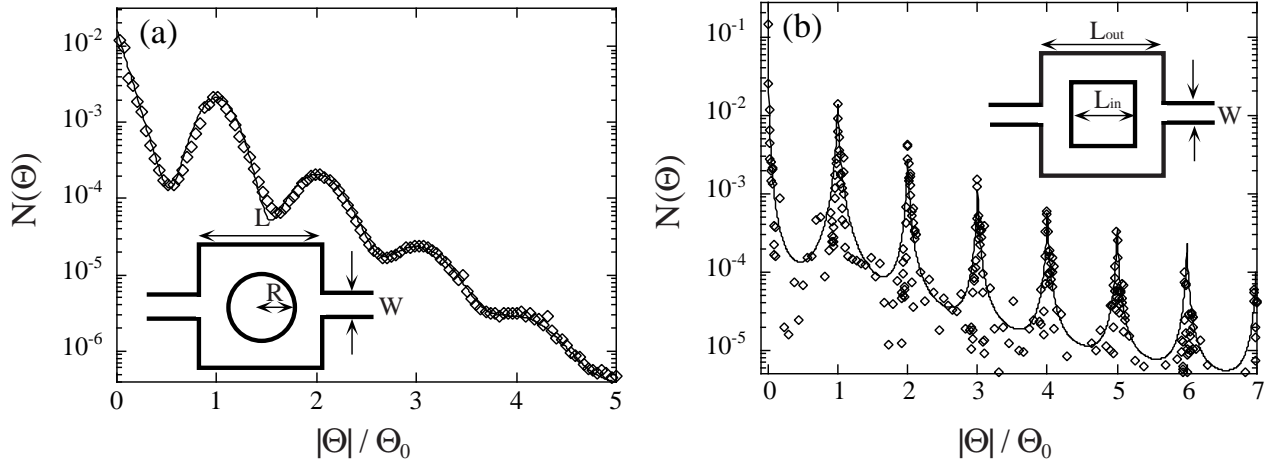


FIG. 1. Semi-logarithmic plot of the effective area distributions in scattering from the (a) Sinai (chaotic) billiard ( $R/W = 3$  and  $L/W = 10$ ) and (b) square AB (regular) billiard ( $L_{in}/W = 6$  and  $L_{out}/W = 10$ ). The numerical simulation results (diamond) for (a) and (b) are well fitted by eqs. (13) and (16) (solid line), respectively. The insets show the schematic views of two types of AB billiards.

For the second term in eq. (14) ( $n > 0$  components), the oscillation amplitude decays exponentially with increasing  $n$ . Therefore, the main contribution to the conductance oscillation comes from the  $n=1$  component, which oscillates with period  $h/2e$ . This behavior is consistent with our previous specific result [i.e., eq. (1)] for the chaotic AB billiard in which magnetic flux penetrates *only* through the hollow [6]. In addition to this property, the oscillation amplitude damps exponentially with increasing magnetic field.

On the other hand, for regular cases (the square AB billiard) the form of  $N(\Theta)$  has been estimated as

$$N(\Theta) \sim n_0(|\Theta| + \Delta_1)^{-z_2} + \sum_{\substack{n=-\infty \\ n \neq 0}}^{\infty} (|n| + n_1)^{-z_1} (|\Theta - n\Theta_0| + \Delta_2)^{-z_2} \quad (16)$$

from the numerical simulation [see Fig. 1(b)]. In the calculation we injected  $9 \times 10^8$  particles into the billiard. In eq. (16)  $n_0, n_1, z_1, z_2, \Delta_1,$  and  $\Delta_2$  are also fitting parameters and  $\Theta_0/2\pi$  is approximately the average area between the outer and inner squares in this case. This distribution leads to [14]

$$\delta\mathcal{R}_D(\Phi) \sim n_0 A_1(\Delta_1, \Phi) + 2A_1(\Delta_2, \Phi) \sum_{n=1}^{\infty} (n + n_1)^{-z_1} \cos\left(4\pi n \frac{\Phi}{\Phi_0}\right), \quad (17)$$

where

$$A_1(\Delta, \Phi) \equiv \int_0^{\infty} dx (x + \Delta)^{-z_2} \cos\left(\frac{4\pi}{\Theta_0} \frac{\Phi}{\Phi_0} x\right). \quad (18)$$

Since  $A_1(\Delta_1, \Phi)$  is equal to the Fourier transform of a power-law function, one can expect a cusplike BWL peak near zero magnetic field [1,15]. In contrast to chaotic cases, the oscillation amplitude decays algebraically for  $n$ . Therefore, we can see that higher-harmonics components give a significant contribution to conductance oscillations. This is because the number of multiple-winding trajectories is much larger in regular billiards than in chaotic billiards.

### III. AAS OSCILLATION AND NEGATIVE MAGNETORESISTANCE

In this section we shall discuss in more detail the difference of  $\delta\mathcal{R}_D(\Phi)$  between chaotic and regular AB billiards. In Fig. 2 we show  $\delta\mathcal{R}_D(\Phi)$  for Sinai (chaotic) and square AB (regular) billiards. The values of the fitting parameters, determined by the classical simulation, are substituted into eqs. (14) and (17). In order to see the marked difference of the  $\Phi$  dependence of  $\delta\mathcal{R}_D(\Phi)$ , we shall investigate the  $n = 0$  term in eqs. (14) and (17), denoted as  $\delta\mathcal{R}_{NMR}(\Phi)$  and the  $n > 0$  term, denoted as  $\delta\mathcal{R}_{AAS}(\Phi)$ , separately, i.e.,

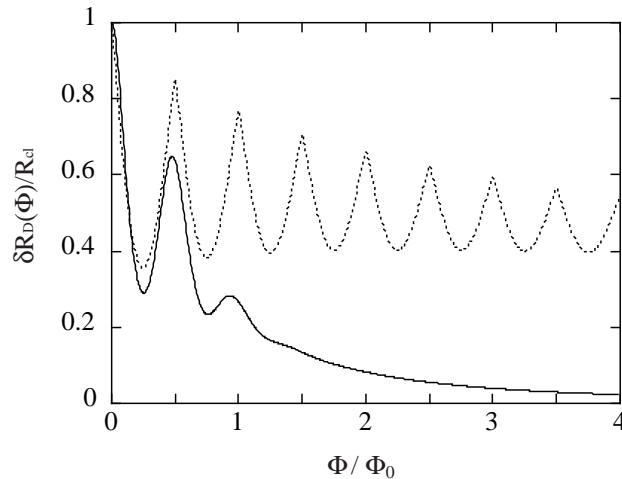


FIG. 2. Semi-classical BWL correction  $\delta\mathcal{R}_D$  to the reflection coefficient for chaotic AB (Sinai) billiard (solid) and regular square AB billiard (dotted) as a function of  $\Phi(= \Theta_0 B/2\pi)$ .  $\delta\mathcal{R}_D$  is normalized to the value at  $\Phi = 0$ , *i.e.*, the classical reflection probability  $\mathcal{R}_{cl}$ .

$$\delta\mathcal{R}_D(\Phi) = \delta\mathcal{R}_{NMR}(\Phi) + \delta\mathcal{R}_{AAS}(\Phi). \quad (19)$$

Figure 3(a) shows  $\delta\mathcal{R}_{NMR}(\Phi)$  which contributes to the negative magnetoresistance for two types of billiards. The shapes of  $\delta\mathcal{R}_{NMR}(\Phi)$  in the vicinity of zero magnetic field are quite different between chaotic and regular billiards, *i.e.*, a quadratic curve versus a linear line [see the inset in Fig. 3(a)]. For large  $\Phi$  (but with the cyclotron radius sufficiently large compared to the system dimension),  $\delta\mathcal{R}_{NMR}(\Phi)$  saturates in chaotic cases, but shows no saturation in regular cases. Similarly, the  $\delta\mathcal{R}_{AAS}(\Phi)$  corresponding to the  $h/2e$  AAS-like oscillation part is indicated in Fig. 3(b). While the oscillation amplitude damps rapidly with increasing  $\Phi$  for the chaotic AB billiard, it damps gently for regular AB billiards.

Therefore, on the basis of the above results, the qualitative difference of  $\delta\mathcal{R}_D(\Phi)$  between chaotic and regular AB billiards is attributed to the different classical distribution of the effective areas. As the dimension of the center obstacle (e.g.,  $R$  for a Sinai billiard and  $L_{in}$  for a square AB billiard) becomes zero, the oscillation structure of  $N(\Theta)$  is indistinct for two types of billiard, so that the  $h/2e$  conductance oscillation would disappear.

To consolidate the above semiclassical prediction of the  $h/2e$  oscillation, we must compare eqs. (14) and (17) with quantum-mechanical calculations (e.g., a recursive Green's function method [16]) and also check the influence of the off-diagonal contribution to  $\delta\mathcal{R}(\Phi)$  [1,7,17]. Moreover, it is desirable to confirm our prediction by having recourse to a random matrix approach for systems with broken time reversal symmetries [18]. Such investigations will be given elsewhere.

#### IV. CONCLUSION

In summary, we have derived the semiclassical formula for  $\delta\mathcal{R}_D(\Phi)$  of single chaotic and regular AB billiards in which a weak  $B$  is applied to the entire region. We have shown that  $h/2e$  oscillations and negative magnetoresistance would appear concurrently in  $\delta\mathcal{R}_D(\Phi)$ : as for  $h/2e$  conductance oscillations, we find the oscillation mainly with a fundamental period  $h/2e$  and rapid damping of the amplitude with increasing  $B$  for the chaotic billiard versus the large contribution of higher harmonic components and mild damping of the oscillation amplitude for a regular billiard; As for negative magnetoresistance, the Lorentzian peak and saturation for the chaotic billiard versus a cusplike structure and no saturation for a regular billiard are reproduced. Although Taylor *et al.* [19] recently made an experimental study of the weak localization peak and self-similar structure of magnetoresistance in a semiconductor Sinai billiard, no detailed experimental result of  $h/2e$  conductance oscillations has yet been reported. We hope that these characteristics of quantum chaos in the quantum magnetotransport will be experimentally observed in ballistic quantum dots forming AB geometry.

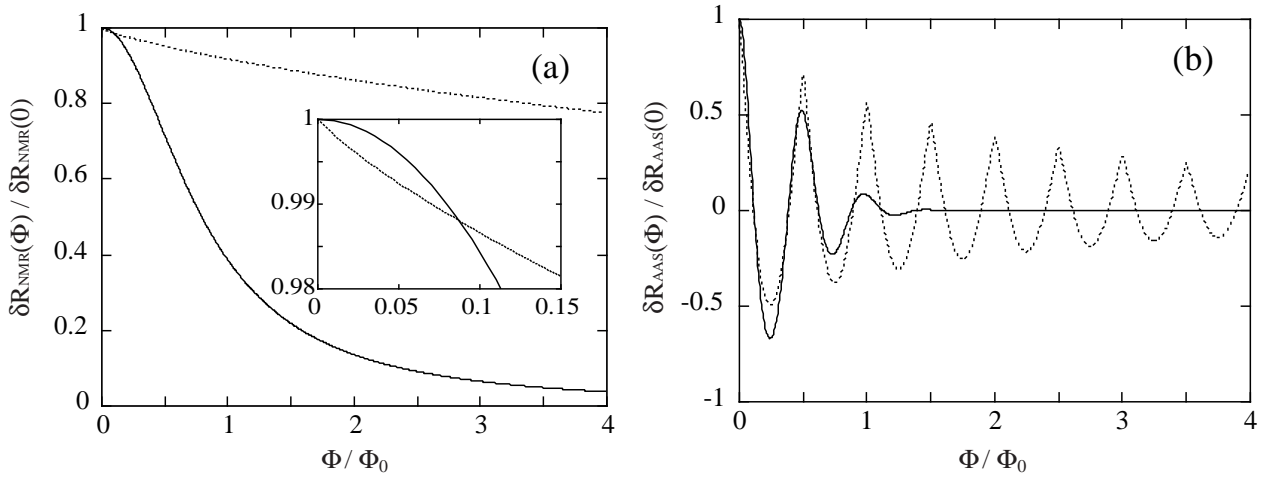


FIG. 3. Magnetic flux dependence of two different components of BWL corrections: (a)  $\delta\mathcal{R}_{NMR}$  contributing to negative magnetoresistance and (b)  $\delta\mathcal{R}_{AAS}$  contributing to the  $h/2e$  oscillation for chaotic (solid) and regular (dotted) AB billiards.  $\delta\mathcal{R}_{NMR}$  and  $\delta\mathcal{R}_{AAS}$  are normalized to the value at  $\Phi = 0$ . The inset in (a) shows  $\delta\mathcal{R}_{NMR}$  in the vicinity of zero magnetic flux.

## V. ACKNOWLEDGEMENTS

We would like to acknowledge Y. Takane, R.P. Taylor, Y. Ochiai, F. Nihey, W.A. Lin, and P. Gaspard for valuable discussions and comments. Numerical calculations were performed on FACOM VPP500 in the Supercomputer Center, Institute for Solid State Physics, University of Tokyo.

- 
- [1] H.U. Baranger, R.A. Jalabert, and A.D. Stone, Phys. Rev. Lett. **70**, 3876 (1993).
  - [2] R.A. Jalabert, H.U. Baranger, and A.D. Stone, Phys. Rev. Lett. **65**, 2442 (1990).
  - [3] For reviews see K. Nakamura, *Quantum versus Chaos: Questions Emerging from Mesoscopic Cosmos* (Kluwer Academic, Dordrecht, 1997); *Chaos and Quantum Transport in Mesoscopic Cosmos*, edited by K. Nakamura, Chaos Solitons and Fractals **8**, No.7/8 (1997).
  - [4] B.L. Altshuler, A.G. Aronov, and B.Z. Spivak, JETP Lett. **33**, 94 (1981).
  - [5] B.L. Altshuler, A.G. Aronov, B.Z. Spivak, D.Yu. Sharvin, and Yu.V. Sharvin, JETP Lett. **35**, 588 (1982); V. Chandrasekhar, M.J. Rooks, S. Wind and D.E. Prober, Phys. Rev. Lett. **55**, 1610 (1985); C.P. Umbach, C. Van Haesendonck, R.B. Laibowitz, S. Washburn and R.A. Webb, *ibid.* **56**, 386 (1986).
  - [6] S. Kawabata and K. Nakamura, J. Phys. Soc. Jpn. **65**, 3708 (1996); Chaos, Solitons and Fractals **8**, 1085 (1997).
  - [7] H.U. Baranger, R.A. Jalabert, and A.D. Stone, Chaos **3**, 665 (1993).
  - [8] M.V. Berry and J.P. Keating, J. Phys. A **27**, 6167 (1994).
  - [9] W.A. Lin, J.B. Delos, and R.V. Jensen, Chaos **3**, 655 (1993).
  - [10] D.S. Fisher and P.A. Lee, Phys. Rev. B. **23**, 6851 (1981).
  - [11] M.C. Gutzwiller, *Chaos in Classical and Quantum Mechanics*, (Springer-Verlag, New-York, 1991).
  - [12] W.A. Lin, Chaos, Solitons and Fractals **8**, 995 (1997).
  - [13] Y.G. Sinai, Russ. Math. Surv. **25**, 137 (1979).
  - [14] Although the arguments leading to eq. (8) must be modified for regular systems [7], we can estimate the BWL correction term in such systems by simply substituting eq. (16) into eq. (8).
  - [15] A.D. Stone, in *Mesoscopic Quantum Physics, Proc. the NATO ASI Les Houches Summer School of Theoretical Physics*, edited by E. Akkermans, G. Montambaux, J.-L. Picherd and J. Zinn-Justin (North Holland, Amsterdam, 1995), pp. 325-371.
  - [16] P.A. Lee and D.S. Fisher, Phys. Rev. Lett. **47**, 882 (1981); T. Ando, Phys. Rev. B. **44**, 8017 (1991).
  - [17] Y. Takane and K. Nakamura, J. Phys. Soc. Jpn. **66**, 2977 (1997).
  - [18] Z. Pulhar, H.A. Weidenmüller, J.A. Zuk and C.H. Lewenkopf, Phys. Rev. Lett. **73**, 21115 (1994); Y.V. Fyodorov, D.V. Savin and H.-J. Sommers, Phys. Rev. E. **55**, R4857 (1997)
  - [19] R.P. Taylor, R. Newbury, A.S. Sachrajda, Y. Feng, P.T. Coleridge, C. Dettmann, N. Zhu, H. Guo, A. Delage, P.J. Kelly, and Z. Wasilewski, Phys. Rev. Lett. **78**, 1952 (1997); M. Fromhold, Nature **386**, 123 (1997).